Preparation of Composite Membranes with Polyimides and Poly(amide–imide)s Skin via Interfacial Condensation for Air Separation

YAW-TERNG CHERN, BAE-SHYANG WU

Institute of Chemical Engineering, National Taiwan Institute of Technology, Taipei, Taiwan 106, Republic of China

Received 14 March 1996; accepted 2 August 1996

ABSTRACT: Composite membranes were prepared by the interfacial condensation of water-soluble diamines with an organic solvent (dichloromethane)-soluble dicarbomethoxy terephthaloyl chloride or carbomethoxy terephthaloyl chloride on top of a porous aluminum oxide support. The morphology of skin on the composite membranes is different in the two different procedures. The polyimide composite membranes with 40-times coatings provide a high gas permeation rate of oxygen and good permselectivity [$\alpha(0_2/N_2)$]. The composite membrane with the polyimides skin at 40-times coatings had a gas permeation rate of oxygen range from 83×10^{-5} to 130×10^{-5} $cm^3(STP)$ $s^{-1}cm^{-2}cmHg^{-1}$, and a permselectivity [$\alpha(O_2/N_2)$] range of 3.57 to 5.60. The composite membrane with poly(amide–imide)s skin at 40-times coatings had a gas permeation rate of oxygen range from 102×10^{-5} to 146×10^{-5} $cm^3(STP)$ s^{-1} cm^{-2} $cmHg^{-1}$, and the permselectivity ($\alpha(O_2/N_2)$) range from 3.20 to 4.96. © 1997 John Wiley & Sons, Inc. J Appl Polym Sci **63:** 693–701, 1997

Key words: composite membrane; interfacial condensation; polyimide; poly(amide–imide); air separation

INTRODUCTION

Stiffer polymers generally have higher mobility selectivity because they behave more like molecular sieves.[1] Also, polymers with high glass transition temperatures can withstand high pressure without resulting in plastic deformation. They are considered important in the separation industry. At high temperatures, aromatic polyimide maintains excellent mechanical properties and chemical stability, so many researchers use polyimides as a separation membrane. This research covers purification and concentration of organic solvents,[2–5] separation of helium and nitrogen,[6] and gas separation.[7–17]

Generally, when membrane for separation is used, it is desirable to have both high permeation and permselectivity. Researchers hoped to build up a composite structure with an ultrathin (less than about 1 μm) dense skin to obtain high permselectivity, while the lower layer is a porous support material to obtain high permeation. This research covers using the interfacial condensation for manufacturing thin film composite,[18–20] an asymmetric coating layer applied to an already formed asymmetric support layer,[21–23] and supporting different siloxane polymers on porous anodic aluminum oxide film.[24,25] There are several advantages in making composite membranes by the interfacial condensation process.[26] The interfacial film that forms the selectively permeable barrier layer can be made quite thin (<0.1 μm). Interfacial condensation also is less susceptible to defect formation in the form of macrovoid pores. Interfacial condensation also permits the making

Correspondence to: Y.-T. Chern.

Contract grant sponsor: The National Science Council, Republic of China.

Contract grant number: NSC 82-0405-E011-049.

of barrier layers that are highly resistant to degradation by exposure to harsh environments. In previous studies,[18–20] the interfacial condensation technique was used mainly for manufacturing thin film composite reverse osmosis membranes. In this research, we attempted to use the interfacial condensation technique for manufacturing composite membranes for air separation. This investigation is a continuation of our previous study on the behavior of interfacial condensation in the synthesis of poly(amic–ester)s. In a previous study,[27] we understood that the interfacial reaction of this system takes place in the organic phase. We also found that the interfacial film itself is not homogenous. The molecular weight of interfacial films decreased gradually in the direction of the thickness from the water phase to the organic phase. Moreover, the morphology of the films changed from dense to porous along the thickness direction of the films. To obtain a homogeneous interfacial film in morphology and molecular weight, the reaction time of interfacial condensation should not exceed 5 min.[28] The chain axis of the poly(amic–ester)s are mainly oriented perpendicularly to the film surface and parallel to the direction of membrane growth.[28] Various polyimides (II) and poly(imide–amide)s (IV) were prepared from dicarbomethoxy terephthaloyl chloride and carbomethoxy terephthaloyl chloride with the corresponding aromatic diamines by using the most favorable conditions for the reaction with 4,4-oxydianiline (Scheme 1). The results of the polycondensation are listed in Table I.[29,30] In this study, we prepare composite membranes by using interfacial condensation on top of a porous aluminum oxide support. Experimental results for the gas permeation rates of the composite membranes are also presented.

EXPERIMENTAL

Materials

Dicarbomethoxy terephthaloyl chloride (DCMTC), carbomethoxy terephthaloyl chloride (CMTC), and 1,6-diaminodiamantane were synthesized as in our previous studies.[31] 1,3-Diaminoadamantane was synthesized according to the method reported elsewhere.[32] 4,4-Oxydianiline(ODA), 4,4-methylene dianiline, 1,4-phenylenediamine, 1,3-phenylene diamine, and 4,4-methylene dianiline were purified by vacuum sublimation. The porous aluminum oxide (1 mm thick with a diameter of 4.6 cm) was obtained from Aucera Technology Corp. The mean diameter of pore size of the aluminum oxide is 0.5 μm measuring on a PMI capillary flow porometer. The porous aluminum oxide was washed using acetone and then vacuum dried at 300°C for 6 h.

Preparation of Composite Membranes

Typical Examples for Preparation of Composite Membranes

We prepared 0.01*M* of dicarbomethoxy terephthaloyl chloride in dichloromethane and 0.01*M* of 4,4-oxydianiline in 10 (v/v)% $DMAc_{(aq)}$ containing 0.002*M* of $Na_2CO_{3(aq)}$. First, one side of the alumina support was soaked in the diamine solution (as shown in Fig. 1). After soaking it for 3 min, we took out the alumina support. Excess solution was drained off the surface by standing the alumina film up. The whole process took 30 s. Next, the surface of alumina containing the diamine solution was soaked in the dichloromethane solution containing dicarbomethoxy terephthaloyl chloride. The interfacial condensation proceeded for 5 min at 5°C, and the composite membrane was then taken from the organic solution. The composite membranes made by interfacial condensation were rinsed with 0.001*N* of $NaOH_{(aq)}$ and then rinsed with deionized water and methanol. The above procedure for preparation of composite membranes was repeated to form multilayer of composite membranes. The membranes were vacuum-dried and then heated in a vacuum oven at 250°C for 5 h, and at 300°C for 2 h, to form imide structure.

Analytical Procedures

Attenuated total reflectance (ATR) spectra were obtained on a Bomen MB 100 Fourier transform infrared spectrometer (FTIR) with 2 cm^{-1} resolution, with KRS-5 used as an internal reflection element. Strips of supported film 4.0 $\times$ 0.5 cm^2 were placed on each side of the crystal so that the film surface was in contact with the crystal face. In a typical experiment, 200 scans per sample were averaged. The electron micrograph was taken with a Hitachi S-2300 scanning electron microscope. The polymer film was coated with gold by sputter deposition prior to the measurement.

Permeation measurements were performed on a Yanaco GTR-10 gas permeability analyzer (Yanaco New Science Ins., Kyoto, Japan) attached to

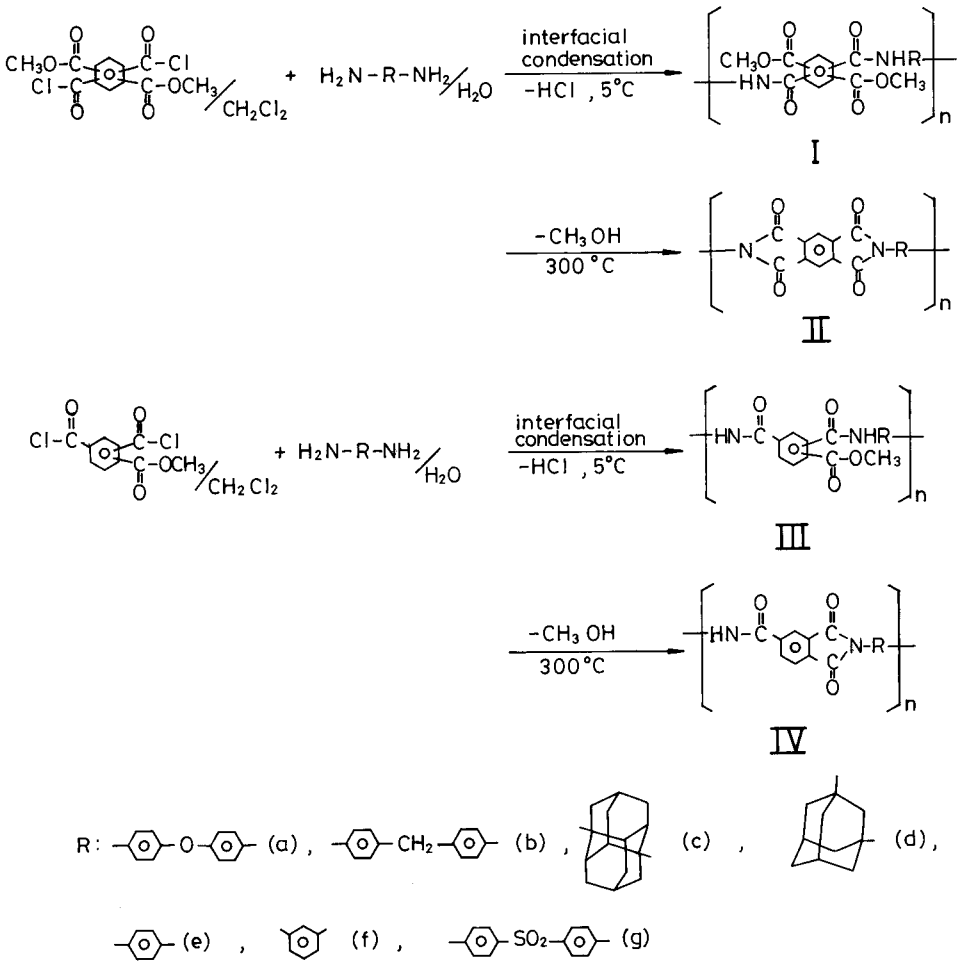

Scheme 1

a Yanaco G-2800T gas chromatograph (GC). The calibration gas was used as an extenal standard for the analysis of the permeative samples. A Yanaco G-2800T GC with thermal conductivity detector (TCD) was used to determine the concentration of permeative gas. The composite membranes to be tested were placed between the two halves of a stainless steel cell held together by bolts with two flat rubber gaskets to ensure a good seal. The effective area available for permeation

Table I Synthesis of Polymers

Polymer	η inh[a](dL/g)	$\overline{Mn}$[b] $\times 10^4$	Polymer	η inh[a](dL/g)	$\overline{Mn}$[b] $\times 10^4$
Ia	0.85	5.5	IIIa	0.36	2.2
Ib	0.53	4.2	IIIb	0.30	1.8
Ic	0.37[c]	—	IIIc	0.29[b]	—
Id	0.24	2.9	IIId	0.17	1.3
Ie	0.45	3.5	IIIe	0.27	2.8
If	0.36	2.1	IIIf	0.20	2.1
Ig	0.27	1.8	IIIg	0.10	1.2

[a] Measured at 30°C at a concentration of 0.5 g/dL in DMAc.
[b] Measured by GPC.
[c] Measured at 30°C at a concentration of 0.5 g/dL in DMAc containing 5 (w/v)% LiCl.

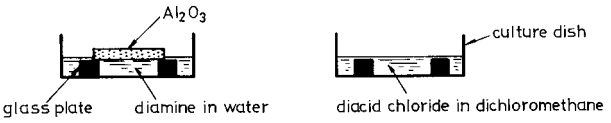

Figure 1 Demonstrative graph for preparation of composite membranes.

was 15.2 cm^2. The gases used in the study were $\geq$99.7% pure. Only pure gas permeation results were measured. The detailed procedure for measuring permeation has been shown in a previous study.[33]

RESULTS AND DISCUSSION

Chemical Structure Analysis by ATR

Comparison of FTIR-ATR spectra of Figure 2(A) and (B) show that the spectra of polyimide II_b has newly added imide characteristic absorption at 1777 cm^{-1} (imide ring C=O), 1369 cm^{-1} (C—N—C, imide), and 723 cm^{-1} (C—N—C, out-of-plane bending imide). In Figure 2(C), for polyimide II_e imide characteristic absorption at 1786, 1359, and 722 cm^{-1} was found. From these results, we understand that the film produced through interfacial condensation is coated on the alumina support film.

Morphology of the Composite Films

The photos of SEM in Figure 3(A,B) show that the difference of morphology was formed by two different procedures. From the photos, we observed that the interfacial film was coated on the alumina support. In Figure 3(A), the alumina support was soaked first in the dichloromethane solution containing DCMTC and then in the $diamine_{(aq)}$. The morphology of the surface of the interfacial film [shown in Fig. 3(A)] is dense and smooth but has a few porous defects. The interfacial film formed was dense and smooth because the interfacial film grew toward the organic phase from the interface region. Thus, the surface in the photo in Figure 3(A) is the surface of the interfacial film adjacent to the water phase. In our previous studies,[27] the surface of the films adjacent to the water phase was dense in morphology. In Figure 3(B), the alumina support was soaked first in the $diamine_{(aq)}$ and then in the dichloromethane solution containing DCMTC. For the same reasoning, the surface in the photo of Figure 3(B) is the surface of interfacial film adjacent to the organic phase. The surface morphology of the interfacial film is dense but uneven [shown in Fig. 3(B)]. The morphology of the interfacial film is consistent with the results of photos of SEM in our previous research.[27] To prepare multilayer composite membranes, we used the procedure in which the alumina support was soaked first in the $diamine_{(aq)}$ and then in the dichloromethane solution containing DCMTC. The main reason for using this procedure is that the uneven surface [shown in Fig. 3(B)] is readily coated new interfacial film. We also found that the thickness of the dense skin in the upper layer of the composite film with 40-times coatings was about 1.2 μm [shown in

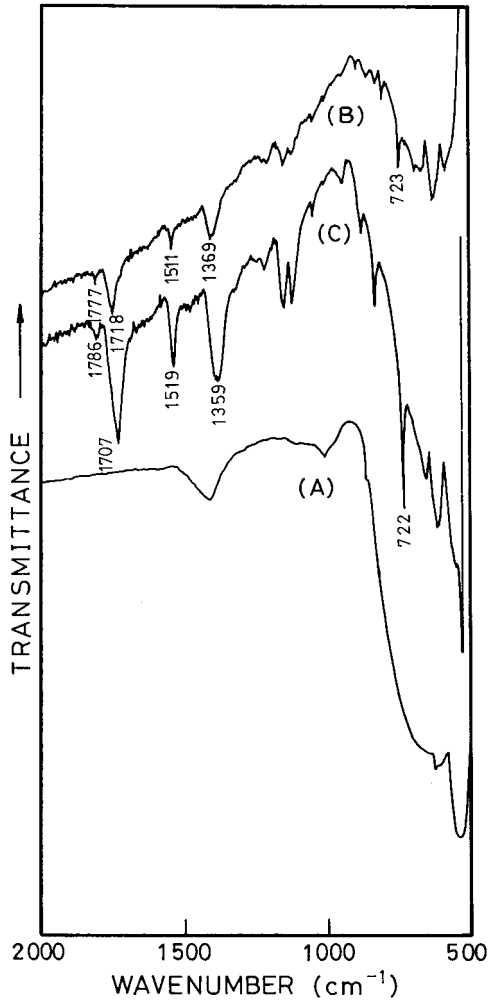

Figure 2 ATR spectra of the polymer composite membranes supported with porous aluminum oxide: (A) bared aluminum oxide, (B) the polyimide II_b composite membrane, and (C) the polyimide II_e composite membrane.

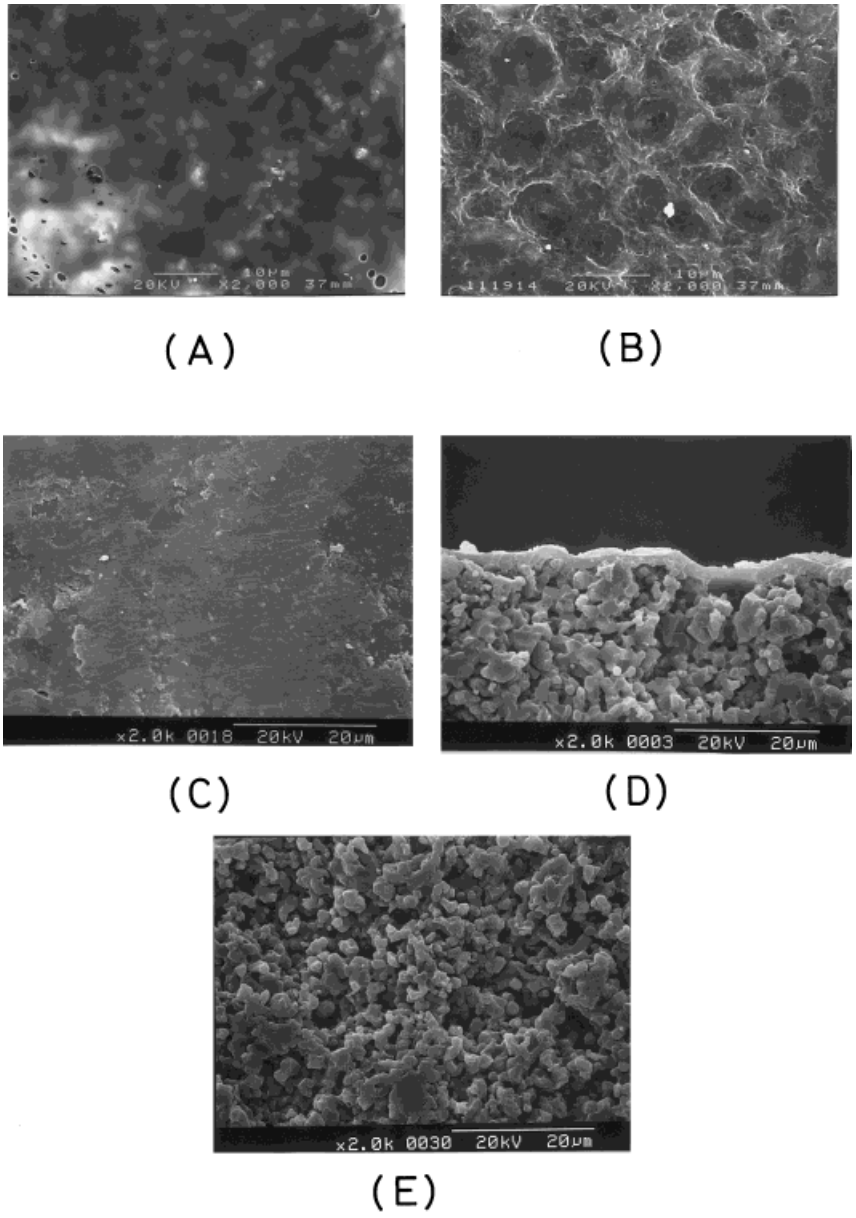

Figure 3 SEM photomicrographs of the polyimide II_a composite membranes. (A) The film was first soaked with DCMTC in dichloromethane solution and then with $ODA_{(aq)}$; first coating, 2000×. (B) The film was first soaked with $ODA_{(aq)}$ and then with DCMTC in dichloromethane solution; first coating, 2000×. (C) A view of skin, 2000×; cross-section at (D), 2000×. Composite film (C) and (D) with 40-times coatings. SEM photography of an aluminum oxide: a view of skin at (E), 2000×.

Figure 3(C,D)]. Figure 3(E) reveals that the aluminum oxide is porous and homogeneous.

The Permeation Rate of Composite Films

Owing to the difficulty in assigning film thickness to the supported membranes, we have chosen to present our results in terms of the permeation rate $\bar{R}$ rather than the permeability. The overall permselectivity of a membrane toward a gas A relative to another gas B is given by an ideal separation factor $[\alpha(A/B)]$, which is defined by the relation

$$\alpha(A/B) = \frac{\bar{R}(A)}{\bar{R}(B)}$$

Table II The Gas Permeation Rates of the Polyimide IIa Composite Films with Multilayer Coatings at 30°C

Time of Coating	$\bar{R}_{CO_2}{}^a \times 10^5$	$\bar{R}_{O_2}{}^a \times 10^5$	$\bar{R}_{N_2}{}^a \times 10^5$	α (O_2/N_2)
0	320	207	85.9	2.41
5	305	188	65.1	2.89
8	293	173	50.0	3.04
11	277	165	50.0	3.30
20	262	140	36.6	3.83
40	205	107	20.0	5.35

Upstream pressure was 16 cmHg.
[a] In cm^3 (STP) s^{-1} cm^{-2} $cmHg^{-1}$.

where $\bar{R}(A)$ and $\bar{R}(B)$ are the mean permeation rates for gases A and B.

Referring to Tables II and III, for both polyimides II_a and II_b composite film systems, the permselectivity ($\alpha(O_2/N_2)$ increases with an increasing number of coatings. On the other hand, the absolute values of the gas permeation rates in both are high, which suggests the efficiency of interfacial condensation as a method to support a thin polymer film. For composite films with the polyimides II_a and II_b at 40-times coatings in Tables II and III, there is high gas permeation rate and permselectivity ($\alpha(O_2/N_2)$. Tables IV and V show the gas permeation rate of the polymer composite membranes at 20-times and 40-times coatings, respectively. Table V shows that the polyimide composite membranes with 40-times coatings provide high permselectivity ($\alpha(O_2/N_2)$ without severely reducing membrane flux. The high gas permeation rate is due to a porous aluminum oxide support and a thin skin layer. The high permselectivity ($\alpha(O_2/N_2)$ is due mainly to the great chain stiffness of the polyimides formed. The gas permeation rate of the composite membrane increases in the order $N_2 < O_2 < CO_2$ with decreasing kinetic sieving diameter, which is commonly observed in gas permeation with polymer materials. At the same diamine moiety, the permselectivity ($\alpha(O_2/N_2)$ of the composite membrane with imide structure (II) was higher than that of the composite membrane with amide-imide structure (IV). This is due to the fact that stiffer polymers generally have a higher mobility selectivity. At the same times coating, among the membranes examined in the present work, the lowest permeation rate was attained with polyimide II_e and poly(amide–imide)s IV_e composite membranes. It is probably because the fact that the main chain with rigid and symmetry of *p*-phenylene diamine is readily packed into the order structure. On the other hand, the permselectivity ($\alpha(O_2/N_2)$ of the composite membrane with polyimides (II) at 40-times coatings, except II_a, increases in the order $II_d < II_g < II_f < II_c < II_e < II_b$ with increasing inherent viscosities of poly(amic–ester)s I (shown in Table I). This is probably due to the fact that the selectivities of the base polymers is used to determine the success of the coating process in forming defect-free films. However, there is no considerable differences in permeation rate values (Table V), changing the amine structure as other reports.[11,12,34]

Table III The Gas Permeation Rates of the Polyimide IIb Composite Films with Multilayer Coatings at 30°C

Time of Coating	$\bar{R}_{CO_2}{}^a \times 10^5$	$\bar{R}_{O_2}{}^a \times 10^5$	$\bar{R}_{N_2}{}^a \times 10^5$	α (O_2/N_2)
0	320	207	85.9	2.41
5	318	194	58.1	3.34
8	310	186	53.0	3.51
11	304	166	47.0	3.53
20	283	156	39.9	3.91
40	233	129	23.0	5.60

Upstream pressure was 16 cmHg.
[a] In cm^3(STP) s^{-1} cm^{-2} $cmHg^{-1}$.

Table IV The Gas Permeation Rates of the Polymers Composite Films with 20-times Coatings at 30°C

Skin	$\bar{R}_{CO_2}{}^a \times 10^5$	$\bar{R}_{O_2}{}^a \times 10^5$	$\bar{R}_{N_2}{}^a \times 10^5$	α (O_2/N_2)
IIa	262	140	36.6	3.83
IIb	283	156	39.9	3.91
IIc	278	152	41.1	3.70
IId	258	132	41.2	3.20
IIe	231	112	34.0	3.29
IIf	244	129	36.8	3.50
IIg	276	146	44.9	3.25
IVa	287	160	47.9	3.34
IVb	296	166	47.0	3.53
IVc	306	175	50.0	3.50
IVd	295	148	50.0	2.96
IVe	258	127	41.0	3.10
IVf	260	134	42.9	3.12
IVg	286	164	53.4	3.07

Upstream pressure was 16 cmHg.
[a] $cm^3(STP)\ s^{-1}\ cm^{-2}\ cmHg^{-1}$.

The reason for this result still remains uncertain. This may be attributable that the influence of permeation rate of composite membranes is complicated. These factors contain the chemical structure, the molecular weight of polymer, morphology, the thickness of skin layer, the interface, and the coating process, etc. In other words, this may be attributed to the fact that the influence of the other factors on permeation rate exceeds the influence of the amine structure on permeation rate. For example, the selectivities of the base polymers is used to determine the success of the coating process in forming defect-free films. Additional work is required to characterize the effect of these factors.

The interfacial polycondensation technique was used in manufacturing composite film, mainly used as reverse osmosis membranes.[26] However, the composite film was used for air separation in the present work. From Tables II and III, the permselectivity ($\alpha(O_2/N_2)$ was not high at five-times coating. These data certainly suggest that the skin layer has defects. The defects can possibly be attributed to the following reasons:

Table V The Gas Permeation Rates of the Polymers Composite Films with 40-times Coatings at 30°C

Skin	$\bar{R}_{CO_2}{}^a \times 10^5$	$\bar{R}_{O_2}{}^a \times 10^5$	$\bar{R}_{N_2}{}^a \times 10^5$	α (O_2/N_2)
IIa	205	107	20.0	5.35
IIb	233	129	23.0	5.60
IIc	245	130	30.0	4.33
IId	217	104	29.1	3.57
IIe	169	83	18.0	4.61
IIf	184	103	24.0	4.29
IIg	223	130	32.0	4.06
IVa	246	143	32.0	4.47
IVb	258	144	29.0	4.96
IVc	265	146	37.0	3.95
IVd	242	127	39.7	3.20
IVe	215	102	25.7	3.97
IVf	239	107	28.0	3.82
IVg	254	128	35.5	3.61

Upstream pressure was 16 cmHg.
[a] $cm^3(STP)\ s^{-1}\ cm^{-2}\ cmHg^{-1}$.

(1) the defects were formed at dry stage; (2) the defects were formed through a thermal treatment; and (3) the defects were formed in the interface between interfacial films. Therefore, the composite membranes with 40-times coating were required for high permselectivity ($\alpha(O_2/N_2)$). From Figure 3(A,B), the surface of interfacial film adjacent to the organic phase is dense but uneven, and the surface of interfacial film adjacent to the water phase is dense and smooth. It is therefore conceivable that the defects were possibly formed in the interface between interfacial films.

A comparison of permeation rate of the systems studied here with other composite membranes was studied by Chung et al.[35] The polyimide composite membrane produced in this work has an oxygen permeation rate that is about four times higher than that of a 6 FDA-durene composite hollow fibers. The permselectivities ($\alpha(O_2/N_2)$) of composite membrane in this work are similar to the corresponding permselectivities for a 6 FDA-durene composite hollow fibers.

CONCLUSIONS

From the chemical structure analysis and photos of SEM, we observed that the interfacial film produced through interfacial condensation was coated on the aluminum oxide support. The morphology of skin on the composite membranes is different in the two different procedures.

The permselectivity ($\alpha(O_2/N_2)$) increases with an increase in the number of coatings due to the fact that pinholes are eliminated by laminating multiple layers to yield separating layers deposited on a porous substrate. The composite membrane with the polyimide at 40-times coatings had a gas permeation rate of oxygen range from 83 $\times 10^{-5}$ to 130 $\times 10^{-5}$ and a permselectivity ($\alpha(O_2/N_2)$) range from 3.57 to 5.60. The composite membrane with the poly(amide-imide)s at 40-times coatings had a gas permeation rate of oxygen range from 102 $\times 10^{-5}$ to 146 $\times 10^{-5}$ cm^3(STP) s^{-1} cm^{-2} cmHg and a permselectivity ($\alpha(O_2/N_2)$) range of 3.20 to 4.96. The permselectivity ($\alpha(O_2/N_2)$) of the composite membrane is different from various diamines. Due to the very thin skin, the thickness of the skin on the composite membranes made by interfacial condensation from various diamines affects the permselectivity of the composite membranes. At the same diamine moiety, the permselectivity ($\alpha(O_2/N_2)$) of the composite membrane with polyimide skin is higher than that of the composite membrane with poly(amide–imide)s skin.

The authors thank manager Stanley C. Chiu. (Aucera Technology Corp.) for providing the aluminum oxide.

REFERENCES

1. S. A. Stern, V. M. Shah, and B. J. Hardy, *J. Polym. Sci., Polym. Phys.,* **25,** 1263 (1987).
2. A. Iwama and Y. Kazuse, *J. Membrane Sci.,* **11,** 297 (1982).
3. C. Blike, K. V. Peinemann, and S. P. Nunes, *J. Membrane Sci.,* **79,** 83 (1993).
4. R. Y. M. Huang and X. Feng, *J. Membrane Sci.,* **84,** 15 (1993).
5. H. Yanagishita, C. Maejima, D. Kitamoto, and T. Nakane, *J. Membrane Sci.,* **86,** 231 (1994).
6. K. V. Peinemann, K. Fink, and P. Witt, *J. Membrane Sci.,* **27,** 215 (1986).
7. Z. Wenle and L. Fengaci, *Polymer,* **35,** 590 (1994).
8. K. C. O'Brien, W. J. Koros, and G. R. Husk, *Polym. Eng. Sci.,* **27,** 211 (1989).
9. W. J. Schell, *J. Membrane Sci.,* **22,** 217 (1985).
10. Y. Maeda and D. R. Paul, *J. Membrane Sci.,* **30,** 1 (1987).
11. S. A. Stern, Y. Mi, and H. Yamamoto, *J. Polym. Sci., Polym. Phys.,* **27,** 1887 (1989).
12. K. I. Okamoto, K. Tanaka, and H. Kita, *J. Polym. Sci. Polym. Phys.,* **27,** 1221 (1989).
13. S. A. Stern, Y. Liu, and W. A. Feld, *J. Polym. Sci. Polym. Phys.,* **31,** 939 (1993).
14. Y. Mi, S. A. Stern, and S. Trohalaki, *J. Membrane Sci.,* **77,** 41 (1993).
15. B. W. Chun, C. Ishizu, H. Itatani, K. Haraya, and Y. Shindo, *J. Polym. Sci. Polym. Phys.,* **32,** 1009 (1994).
16. M. R. Coleman, R. Kohn, and W. J. Koros, *J. Appl. Polym. Sci.,* **50,** 1059 (1993).
17. G. Zoia, S. A. Stern, A. K. St. Clair, and J. R. Pratt, *J. Polym. Sci. Polym. Phys.,* **32,** 53 (1994).
18. J. E. Cadotte, U.S. Pat. 4,277,344 (1981).
19. J. E. Cadotte, R. J. Petersen, R. E. Larson, and E. E. Erickson, *Desalination,* **32,** 23 (1980).
20. R. E. Larson, J. E. Cadotte, and R. J. Petersen, *Desalination,* **38,** 473 (1981).
21. H. Makino, Y. Kusuki, T. Harada, H. Shimazaki, and T. Isida, U.S. Pat. 4,528,004 (1985).
22. H. Makino, Y. Kusuki, T. Harada, H. Shimazaki, and T. Isida, U.S. Pat. 4,440,643 (1984).
23. B. Bikson and J. Nelson, U.S. Pat. 4,826,599 (1989).
24. S. Sugawara, M. Konno, and S. Saito, *J. Membrane Sci.,* **44,** 151 (1989).
25. S. Sugawara, M. Konno, and S. Saito, *J. Membrane Sci.,* **43,** 313 (1989).

26. G. Y. Chai and W. B. Krantz, *J. Membrane Sci.,* **93,** 175 (1994).
27. Y. T. Chern and B. S. Wu, *J. Appl. Polym. Sci.,* **61,** 1853 (1996).
28. Y. T. Chern, B. S. Wu, and C. M. Huang, *Polym. Bull.,* **36,** 609 (1996).
29. Y. T. Chern, *Makromol. Chem. Phys.,* **196,** 3217 (1995).
30. Y. T. Chern, *J. Polym. Sci., Polym. Chem. Ed.,* **34,** 133 (1996).
31. Y. T. Chern and J. J. Wang, *Tetrahedron Lett.,* **36,** 5805 (1995).
32. G. W. Smith and H. D. Williams, *J. Appl. Polym. Sci.,* **26,** 2207 (1961).
33. Y. T. Chern and L. W. Chen, *J. Appl. Polym. Sci.,* **44,** 1087 (1992).
34. L. M. Robeson, W. F. Burgoyne, M. Langsam, A. C. Savoca, and C. F. Tien, *Polymer,* **35,** 4970 (1994).
35. T. S. Chung, E. R. Kafchinski, and R. Vora, *J. Membrane Sci.,* **88,** 21 (1994).